Holographic properties of doubly doped lithium niobate crystals with Indium

Qingsheng He, Yunbo Guo*, Yi Liao, Liangcai Cao, Guodong Liu, and Guofan Jin
State Key Laboratory of Precision Measurement Technology and Instruments,
Tsinghua University, 100084 Beijing, China

ABSTRACT

The holographic properties of doubly doped lithium niobate crystals with Indium have been investigated. It is found that doping slight Indium concentration (0.5mol%) in $LiNbO_3$:In, Fe crystal can efficiently increase the sensitivity with small dynamic range changing. To improve the whole holographic properties of $LiNbO_3$ crystal, $LiNbO_3$:In, Fe with ideal doping concentrations and a new photorefractive material $LiNbO_3$:In, Mn have been proposed and achieved larger dynamic range, higher sensitivity and better signal-to-noise ratio than $LiNbO_3$:Fe crystal (Fe:0.03wt.%) that is generally considered as a preferable storage medium in holographic memories. In a common volume of $LiNbO_3$:In, Fe crystal proposed, 2030 holograms have been successfully multiplexed and exactly identified in a compact volume holographic data storage and correlation recognition system.

Keywords: Holographic properties; $LiNbO_3$:In, Fe crystal; $LiNbO_3$:In, Mn crystal; Holographic memories.

1. INTRODUCTION

Volume holographic memories have attracted intense interest because of their potential in high capacity storage, fast parallel process and content addressability [1, 2]. To a large extent, the system performances depend on the properties of storage media. For holographic storage materials, two of the most important parameters are dynamic range (*M/#*) and sensitivity (*S*). In addition, low scattering will result in high signal-to-noise ratio (SNR) [1, 3, 4].

Photorefractive lithium niobate ($LiNbO_3$) crystal has been widely investigated for applications in holographic data storage. Usually transition-metal dopants, such as Fe, Cu, Ce and Mn, are added to the melt to improve the photorefractive effect. And Fe is most effective in producing large improvements in both dynamic range and sensitivity [5]. Many successful demonstrations of holographic storage systems have been achieved in $LiNbO_3$:Fe crystals [1, 6]. One approach to boosting the *M/#* and sensitivity for Fe-doped $LiNbO_3$ crystal is to increase the Fe doping level. However, the higher the concentration of Fe, the larger the photorefraction effect will be. The characteristic will cause strong scattering noise harmful for holographic storage. Thus a trade-off between *M/#*, *S* and SNR has to be considered when we design $LiNbO_3$:Fe crystals for holographic applications, and 0.03wt.% Fe has been generally considered as a preferable doping concentration for high-capacity holographic data storage. In addition, due to the dark-decay mechanism, there is a limit on the highest practical doping level 0.06 wt.% for $LiNbO_3$:Fe crystal and any further

* guoyb98@mails.tsinghua.edu.cn; Tel: 86-10-62781204; fax: 86-10-62784503.

Holography, Diffractive Optics, and Applications II, edited by Yunlong Sheng, Dahsiung Hsu, Chongxiu Yu, Byoungho Lee, Proceedings of SPIE Vol. 5636 (SPIE, Bellingham, WA, 2005) · 0277-786X/05/$15 · doi: 10.1117/12.580933

increase of the doping level above this limit cannot result in larger *M/#* and sensitivity [7]. However, Manganese (Mn) center has a deeper energy level than Fe center, and is experimentally found that the highest practical doping level in Mn-doped $LiNbO_3$ is ~0.5wt.% $MnCO_3$, which promises larger *M/#* and sensitivity [4, 8].

It is well known that damage-resistant dopants (e.g., Mg, Zn, In, etc.) have been doped in $LiNbO_3$ crystal to reduce optical damage [9~11]. Among them, In impurity is the most "efficient" due to the lowest threshold concentration which was reported about 1.5~2.0mol.%. Volk *et al.* [9, 10] detailedly analyzed the properties of In-doped $LiNbO_3$ crystals. Qiao *et al.* [12] got a high sensitivity of photorefractive effect in $LiNbO_3$:In crystal, and the significant suppression of the photorefractive light-induced scattering has been observed in $LiNbO_3$:In, Fe crystal [11]. All these experiments show that doping Indium is a very efficient way to increase the photorefractive sensitivity and the damage-resistance ability of $LiNbO_3$ crystal. However, the photorefraction is inversely proportional to the photoconductivity [9], so it is difficult to get high *S* and SNR simultaneously with large *M/#* in singly doped $LiNbO_3$:In crystal.

Therefore, it is expected that doubly doped $LiNbO_3$:In, Fe (or $LiNbO_3$:In, Mn) crystal combining with the advantages of In doping with Fe (or Mn) doping is a promising photorefractive material for holographic applications. In this paper, we will firstly investigate the properties of $LiNbO_3$:In, Fe crystals with a series of In doping concentrations. Next, based on synthesizing the effects of In doping and Fe (or Mn) doping, $LiNbO_3$:In, Fe with ideal doping concentrations and a new photorefractive material $LiNbO_3$:In, Mn are proposed to improve the whole holographic properties of $LiNbO_3$ crystal. Moreover, two samples proposed have been grown and compared with $LiNbO_3$:Fe crystal (Fe:0.03wt.%) under the same experimental conditions. Finally, we applied this proposed $LiNbO_3$:In, Fe crystal to a compact volume holographic data storage and correlation recognition system and got excellent performances.

2. EXPERIMENTS ON THE EFFECT OF INDIUM DOPING

In the experiments, we used four congruently melting $LiNbO_3$:In, Fe samples whose concentrations of In were 0.5, 1, 2 and 3mol% in the melt, which we referred to as InFe1, InFe2, InFe3 and InFe4. For comparison, a sample of single doped $LiNbO_3$:Fe crystal (referred as Fe1) was also investigated. All samples have the same Fe concentration of 0.03wt%, the grown state and the dimensions of 10×10 (thickness)×10mm^3. Additionally, these samples are 45°-cut and polished to optical quality.

The experimental setup is a typical 90°-geometry system. A He-Ne laser beam at the wavelength of 632.8nm was used to record and erase holograms. To get the maximum dynamic range and sensitivity, the crystals were immersed in a sodium chloride solution which was used to minimize the influence of the photovoltaic field [13, 14], and then placed on a rotation stage. The light beam with a diameter of 4mm was split by the PBS into two equal-intensity beams as a reference beam and an object beam. The grating vector was always aligned along the *c* axis. During recording, the object beam was blocked from time to time to measure the holographic diffraction efficiency as the ratio of diffracted and incident light intensities. After the grating reached the saturation, we used Bragg-mismatched erasure [8], i.e., during erasure the sample was rotated far away from the Bragg-matched position and illuminated by the same two beams to record holograms. In order to avoid building another strong hologram, the sample was rotated 0.02° every 10s during erasure. At the end of each period of erasure, the diffraction efficiency was measured by scanning over an adequate range of angle and finding the maximum diffraction efficiency with the only reference beam on.

Figure 1 shows a typical recording and erasing behavior of the single grating in $LiNbO_3$:In, Fe crystal. The temporal trace of η during recording and erasing could be well described by functions given

by $\eta(t)=\sin^2\{(\pi\Delta n_{sat}L/\lambda\cos\theta)[1-\exp(-t/\tau_r)]\}$ and $\eta(t)=\sin^2\{(\pi\Delta n_0 L/\lambda\cos\theta)\exp(-t/\tau_e)]\}$, respectively. Here θ is the incident angle inside the crystal, τ_r, τ_e are the recording and erasing time constants, λ is the wavelength outside the crystal, Δn is the amplitude of refractive-index change, and L is the effective interaction length. In addition, *M/#*, *S* can be defined as $M/\#=(A_0/\tau_r)\tau_e$ and $S=(A_0/\tau_r)/(IL)$, where $A_0=\pi\Delta n_{sat}L/(\lambda\cos\theta)$, and I is the total incident recording intensity [3, 4]. Therefore, a good fit between experimental data and functions of the diffraction efficiency indicates that the values of *M/#*, *S* can be well obtained by the experimental curves.

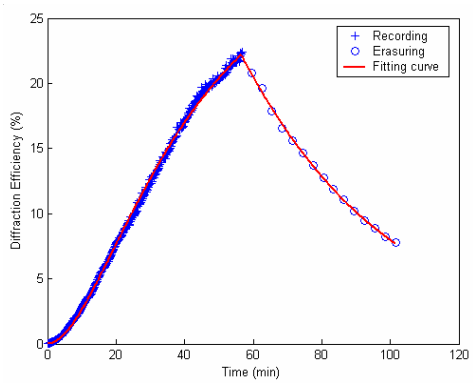

Fig.1 Experimentally measured and fitting curves of $LiNbO_3$:In,Fe(In:2mol%,Fe:0.03wt.%) crystal.

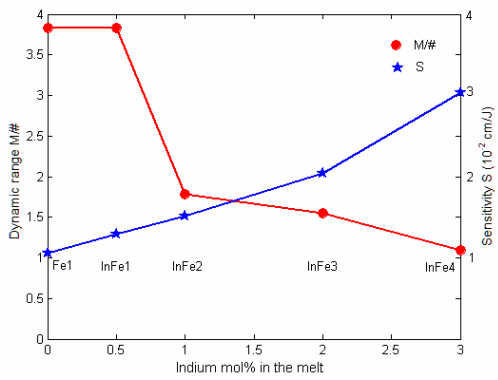

Fig2. Dynamic range *M/#* and sensitivity *S* of $LiNbO_3$:In, Fe crystals versus In doping concentrations.

Figure2 illustrates the dependences of measured *M/#* and *S* of $LiNbO_3$:In, Fe crystal on In doping concentrations. Different In concentrations correspond to different samples. The asterisk signs describe the sensitivity and show that *S* increases similarly linearly with the increase of In concentration under 2mol% i.e., the threshold concentration of In-doped $LiNbO_3$ crystal. However, when In concentration increases to 3mol%, the sensitivity sharply improves with the increasing ratio twice as large as that of the threshold concentration below. In addition, the dot signs represent dynamic range, and *M/#* decreases with In concentration increasing, but it is surprising that InFe1 has an identical value of *M/#* with Fe1. And *M/#* changes sharply when In concentration is improved from 0.5mol% to 1mol% and from 2mol% to 3mol%. Comparing the properties of InFe1 with InFe4, we can find that *S* has a sharp increase by a factor of 2.3, but *M/#* strongly decreases by a factor of 3.5.

Holographic properties of $LiNbO_3$ crystal mainly depend on photorefractive centers. In doubly doped $LiNbO_3$:In, Fe crystal, In ions do not participate in the charge transport and simply affect concentrations and incorporation of other ions which contribute to the photoconductivity [5]. When In concentration is below the threshold, In ions incorporate onto Li-sites, removes Nb_{Li} and also substitute both for Fe^{2+} and Fe^{3+}. Therefore the photoconductivity σ increases due to a reduction of Nb_{Li} and a variation of the ratio Fe^{2+}/Fe^{3+}. The increase of σ will cause time constants τ_r, τ_e to reduce. Though A_0 reduces too, A_0/τ_r is still improved due to the sharp increase of σ. So the sensitivity increases with In concentrations under 2.0mol% shown as Fig.2. Generally τ_r, τ_e change at the same magnitude for $LiNbO_3$:Fe crystal [15]. However, the asymmetry in the reduction of time constants exists for $LiNbO_3$:In, Fe crystal, which can be explained in terms of a multiple-defect-center model [16]. When In concentration is above 0.5mol%, a complete disappearance of Nb_{Li} from $LiNbO_3$:In, Fe crystal perhaps happens [10], and the asymmetry disappears. With a decrease of A_0, *M/#* will decrease dramatically. When In concentration is beyond the threshold, In ions incorporate both onto Li

(In_{Li}) and Nb (In_{Nb}) sites, and Fe^{3+} incorporates mainly onto the Nb-sites, loosing its acceptor properties. It will result in a sharp increase of photoconductivity, and *M/#, S* change greatly.

Therefore, slightly In doping (such as 0.5mol%) under the threshold concentration in $LiNbO_3$:In, Fe crystal could be a good advice to improve the sensitivity with small *M/#* changing.

3. IMPROVEMENT OF HOLOGRAPHIC PROPERTIES OF LINBO$_3$:IN, FE CRYSTAL

Due to the trade-off between *M/#*, *S* and SNR, $LiNbO_3$:Fe crystal with 0.03wt.% Fe has been generally considered as a preferable storage medium for volume holographic data storage. Nevertheless, for practical holographic applications, larger dynamic range and higher sensitivity are required, and it is always attracting to dope the highest possible Fe concentration in $LiNbO_3$ crystal. Since there is a limit on the highest practical doping concentration (0.06wt.%) of Fe:$LiNbO_3$ for electron tunneling effect [7], and any further increase of the doping concentration beyond the limit cannot result in larger *M/#* and sensitivity, 0.06wt% Fe is an ideal doping concentration for the improvement of the holographic properties of $LiNbO_3$ crystal [7, 15].

Obviously, if Fe concentration directly increases to 0.06wt.%, the scattering noise will increase and can not be suitable for holographic applications. As discussed in section 2, slightly In doping (0.5mol% In) in $LiNbO_3$:Fe crystal is an efficient way to solve the problem. On one hand, In doping can greatly reduce the scattering noise caused by the increase of Fe doping, that is to say, In doping makes it possible to dope high Fe concentration in $LiNbO_3$ crystal with the assurance of a suitable SNR. On the other hand, In doping also improves the sensitivity of $LiNbO_3$ crystal. Meantime, the value *M/#* is perhaps reduced by slightly In doping at a certain degree compared with $LiNbO_3$:Fe crystal (Fe:0.06wt.%), but it still increases compared with $LiNbO_3$:Fe crystal (Fe:0.03wt.%). Therefore, the whole holographic properties of $LiNbO_3$ crystal will be improved.

In addition, *M/#* and *S* in Fe-doped $LiNbO_3$ crystals are strong functions of the oxidation state [15, 17, 18]. Typically, the more the crystal is reduced, the larger the sensitivity will be. However, too large absorption coefficient α which is related to the oxidation state [15], will greatly shorten the storage time. Moreover, there exists an optimal value α for maximum *M/#*. A theoretical model has been developed and shown that the optimum α for the crystal with thickness d is $\alpha d = 1$ [17]. So a suitable oxidation state is needed to get excellent holographic properties.

According to the guide line above, $LiNbO_3$:In, Fe crystal with 0.5mol% In, 0.06wt.% Fe is grown (referred as InFe5). The dimension is $20\times20\times30mm^3$. After thermal annealing it is slightly oxidized with $\alpha \approx 0.25cm^{-1}$ at $\lambda = 632.8nm$ and $\alpha \approx 0.5cm^{-1}$ at $\lambda = 532nm$. Figure 3 shows InFe5 measured and fitting curves under the same experimental conditions with section 2. For comparison, Fe1 is also described.

From the single-hologram recording and erasure curve, we can calculate *M/#*, *S* and Δn_{sat}. Table1 describes these photorefractive parameters of Fe1&InFe5 crystals.

Table1 Photorefractive properties of Fe1&InFe5 crystals

Sample	$\eta_m(\%)$	*M /#*	$S(10^{-2}cm/J)$	$\Delta n_{sat}(10^{-5})$
Fe1	36	3.83	1.05	2.50
InFe5	61	7.47	1.98	3.59

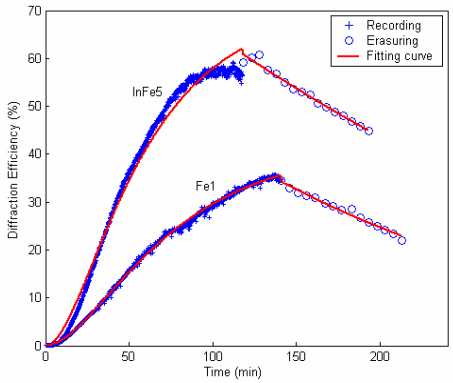

Fig.3 Experimentally measured and fitting curves of $LiNbO_3$:In, Fe(InFe5) and $LiNbO_3$:Fe (Fe1) crystals.

Note that *M/#* is proportional to the effective interaction length L [1, 3]. The values of L for Fe1 and InFe5 are both 4mm, so the value *M/#* can be directly comparable. The results show that InFe5 has larger diffraction efficiency. A larger Δn_{sat} results from the increase of Fe doping, and slightly In doping causes that the increase of Δn_{sat} is less than twice. All that makes InFe5 crystal achieve the values $M/\# = 7.47$ and $S \approx 0.02 cm/J$, twice as large as those of Fe1.

Furthermore, we performed a holographic image storage experiment to evaluate the scattering characteristics of InFe5 crystal and Fe1 crystal. An argon-ion laser beam with the wavelength of 514nm was used to store and retrieve holograms in a 90° geometry system. The reconstructed holograms are shown in Figure 4, from which we can see that the reconstructed hologram from InFe5 has a quite high SNR and even better than that from Fe1.

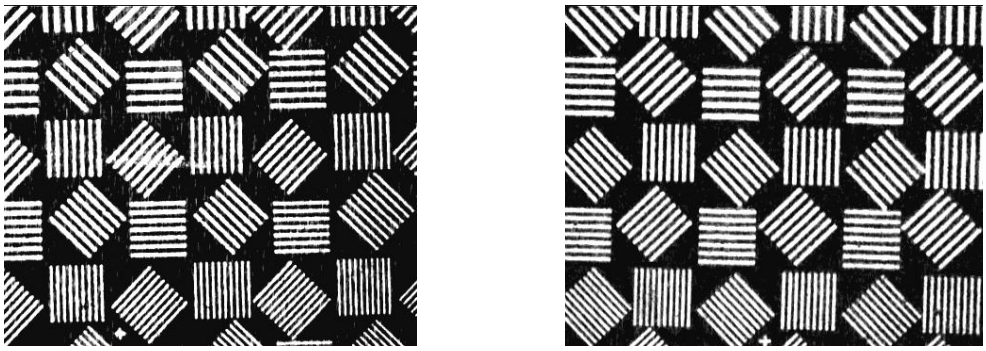

(a) (b)

Fig.4. The reconstructed hologram from the sample of: (a) $LiNbO_3$:Fe crystal; (b) $LiNbO_3$:In, Fe crystal.

In summary, we have grown a sample of $LiNbO_3$:In, Fe crystal with 0.5mol%In, 0.06wt.%Fe and slightly oxidized state, and achieved larger *M/#*, higher *S* and better SNR than $LiNbO_3$:Fe crystal with 0.03wt.%Fe under the same experimental conditions.

4. HOLOGRAPHIC PROPERTIES OF $LINBO_3$:IN, MN CRYSTAL

It is well known that Mn center is deeper than Fe center, thus the electron tunneling effect in Mn-doped $LiNbO_3$ crystal is smaller [4], and it is possible to use $LiNbO_3$:Mn with higher doping levels for holographic storage to get larger *M/#*

and sensitivity. Yang *et al* has investigated $LiNbO_3$:Mn crystals with the doping levels of 0.2at.%Mn and 0.5wt%$MnCO_3$, and found that these crystals have very large *M/#* and sensitivity with little holographic scattering [4, 7]. If we dope slight In concentration into $LiNbO_3$:Mn crystal as section 3, the sensitivity will further increase and the scattering will be less, with small *M/#* changing. The new photorefractive material $LiNbO_3$:In, Mn promises to have larger *M/#*, *S* and less scattering than $LiNbO_3$:Fe crystal.

A sample of $LiNbO_3$:In, Mn crystal with In:0.5mol%, Mn:0.2at.% and as-grown state (referred as InMn1) was used to investigate the holographic properties of this new material. The dimension is $10\times10\times10mm^3$. For deep center Mn, the cut-off wavelength of *D*-band is about 520 nm [19], so an argon-ion laser beam with the wavelength of 514nm was used to perform holographic grating experiments in the same 90^o geometry system as section 2. $LiNbO_3$:Fe crystal (Fe1) is also tested for comparison under the same experimental conditions.

Fig.5 describes the holographic grating recording and erasing behaviors of InMn1 and Fe1 crystals respectively.

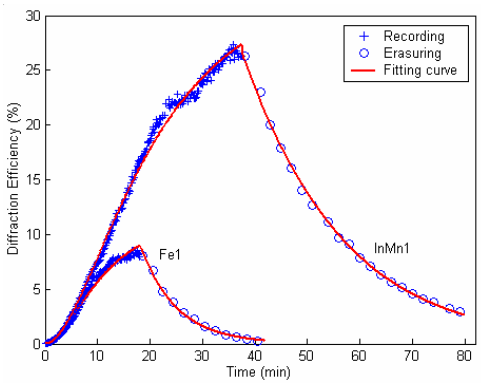

Fig.5 Experimental measured and fitting curves of $LiNbO_3$:In, Mn and $LiNbO_3$:Fe crystals.

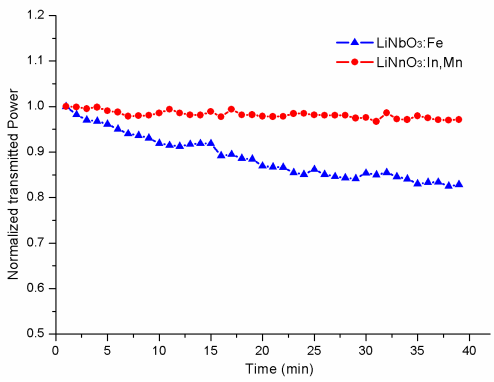

Fig.6 The scattering behavior measurements of $LiNbO_3$:In, Mn and $LiNbO_3$:Fe crystals.

The calculated values from the curves are listed in Table2, from which we can see that InMn1 has the diffraction efficiency three times as that of Fe1, larger *M/#*, Δn_{sat} and higher *S*. Though the bulk photovoltaic coefficient of Mn is smaller than that of Fe in $LiNbO_3$ crystals, the higher doping level makes $LiNbO_3$:In, Mn crystal get better holographic performances than $LiNbO_3$:Fe crystal.

Table2 Holographic properties of Fe1&InMn1 crystals

Sample	$\eta_m(\%)$	$M/\#$	$S(10^{-2}cm/J)$	$\Delta n_{sat}(10^{-5})$
Fe1	8.8	0.58	1.27	0.90
InMn1	27.4	1.35	1.40	1.56

In addition, we also performed an experiment to quantitatively assess the scattering behavior of InMn1 and Fe1 with the same thickness [4]. We used the Ar^+ laser beams with the wavelength of 514nm and the average intensities in the cases were $180mW/cm^2$. The transmission light spot of InMn1 didn't change, while that of Fe1 crystal dispersed out. And their normalized transmitted powers are plotted as a function of time in Fig.6. The results show that InMn1 has a very high damage-resistant ability and the holographic scattering in InMn1 builds up far slower than in Fe1.

The experimental results above prove that InMn1 has better holographic properties than Fe1. We expect that the performance of $LiNbO_3$:In, Mn crystal for holographic applications can be improved further by use of the optimal

recording wavelength 458nm for Mn-doped $LiNbO_3$ crystal [4], optimizing the material with larger Mn concentration (0.5wt.% $MnCO_3$) and highly oxidized state, transmission recording geometry, or a combination of these procedures.

5. APPLICATIONS IN HOLOGRAPHIC MEMORIES

To further investigate holographic properties of doubly doped $LiNbO_3$ with Indium, we applied InFe5 crystal (In:0.5mol%, Fe:0.06wt.%, slightly oxidized state) to a compact volume holographic data storage and correlation recognition system. This system is a typical 90^o-geometry recording setup. A diode-pumped solid-state laser ($\lambda = 532nm$) is used as the light source, and all of the holograms are angular-fractal multiplexed in a coherent volume of the crystal which is immersed in a sodium chloride (NaCl) solution to minimize the influence of the photovoltaic field on the multiplexed holograms. Inputting an original image to illuminate the coherent volume, we can get the correlation results of the image with all stored holograms with a charge coupled device (CCD). A holographic diffuser is put just before the spatial light modulation (SLM, 1024×768 pixels, $26\times26\mu m^2$) to suppress the sidelobes of correlation patterns and the cross-talk noise caused by them [20].

Recently we have achieved good experimental results in $LiNbO_3$:Fe crystal (Fe:0.03wt%, grown state, $17\times17\times25mm^3$, referred as Fe2) in this system [21]. Experiments show that InFe5 crystal has a maximum tolerable exposure time of 15s larger than 10s in Fe2, and a minimum tolerable exposure time of 0.8s smaller than 1.3s in Fe2, which is due to its larger dynamic range and higher sensitivity than Fe2 crystal. It is expected that better performances will be achieved in InFe5.

In order to realize high capacity holographic storage in InFe5 crystal, an appropriate exposure time schedule must be designed according to the characteristics of the crystal and the system. The often adopted original time schedule put forth by Psaltis *et al* [22], is based on the invariability of writing- and erasure-time constants. In our system, the holographic diffuser is very effective to improve the recognition accuracy, but it brings a serious problem that the object beam becomes quite weak after passing through the diffuser, which causes that recording a hologram will need longer exposure time, and the whole recording time will greatly increase. What's worse, long exposure time will cause the dynamic increase of photoconductivity resulting from the increase of the electrons in the conduction band with the illuminating time and the gradual increase of the photovoltaic electric current which forms a circuit in NaCl solution. The change of the photoconductivity will cause the dynamic reduction of time constants. And the previously stored holograms will be badly erased under the original time schedule. Derived from the original time schedule model, the exposure time of each hologram in the same horizontal direction (called a row) varies approximately according to the exponential function with a decay constant that increases by the number of holograms in the row. We amended the time schedule by multiplying the decay constant of each row with a restraint factor that changes referencing to the recorded result of the last row. The adaptable restraint factor compensates for the dynamic change of time constants, and the new restrictedly gradually-reduced exposure time schedule promises to equalize the diffraction efficiency of all stored holograms.

With the new exposure time schedule, in a coherent volume of $0.074cm^3$ in InFe5 crystal, we have successfully multiplexed 2030 images using 70 angles in the horizontal direction and 29 lines in the vertical direction. The longest exposure time is 10s, while the shortest is 0.9s, and the whole recording time is 91min, 13.3% shorter than that in Fe2 crystal which has achieved the same storage capacity. Figure 5 shows the correlation spots array of the 2030 holograms read by a white blank. There is an approximately uniform diffraction efficiency except a few images which are not well

recorded because of the inaccuracy of the shutters. Inputting the original image one by one, we can get the correlation recognition results of all 2030 holograms. The correlation accuracy is about 98.4%, which also indicates that almost of 2030 holograms have been recorded well and the storage density of $21 Gbits/cm^3$ has been achieved in $LiNbO_3$:In, Fe crystal.

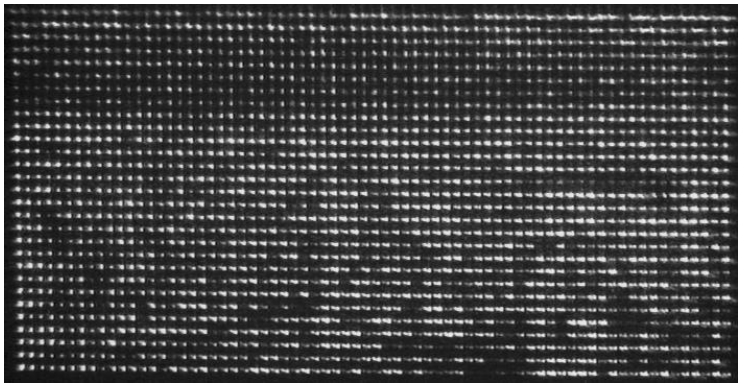

Fig.5 The correlation spots array of the 2030 holograms read by a white blank in $LiNbO_3$:In, Fe crystal (70×29).

6. CONCLUSIONS

In conclusions, we have shown that doubly doped $LiNbO_3$ with Indium is very promising for holographic recording. Slightly In doping concentration (such as 0.5mol%) under the threshold concentration can efficiently improve the sensitivity and SNR with *M/#* changed little. Two ways have been proposed to improve the holographic properties of $LiNbO_3$ crystals, and $LiNbO_3$:In, Fe crystal (In:0.5mol%, Fe:0.06wt.%) and $LiNbO_3$:In, Mn (In:0.5mol%, Mn: 0.2at.%) have got larger dynamic range, higher sensitivity and better signal-to-noise ratio than Fe:$LiNbO_3$ crystal (Fe:0.03wt.%). Furthermore, in this proposed $LiNbO_3$:In, Fe crystal, a high-density holographic data storage has been achieved with the high recognition accuracy. We believe that doubly doped $LiNbO_3$ crystal tailored by slightly damage-resistant dopant Indium doping, highly effective photorefractive centers Fe or Mn doping and suitably thermal annealing, will be a very promising photorefractive material for large density, fast access and high SNR holographic memories.

ACKNOWLEDGMENT

This work was supported by National Natural Science Foundation of China (No. 60277011) and National Research Fund for Fundamental Key Projects NO.973 (G19990330).

REFERENCES

1. H. J. Coufal, D. Psaltis, and G. T. Sincerbox, Holographic Data Storage (Springer, New York, 2000).
2. G. W. Burr, S. Kobras, H. Hanssen, and H. Coufal, "Content-addressable data storage by use of volume holograms," Appl. Opt. **38**, 6779-6784 (1999).
3. S. Tao, M. Lee, K. Kitamura, H.Hatano, L. Galambos, L. Hesselink, "Holographic properties of doped stoichiometric $LiNbO_3$ crystals," in Fifth International Symposium on Optical Storage, F. Gan and L. Hou, eds., Proc. SPIE, **4085**, 46-50 (2001).

4. Y. Yang, I. Nee, D. Psaltis, M. Luennemann, D. Berben, U. Hartwig and K. Buse, "Photorefractive properties of lithium niobate crystals doped with manganese," J. Opt. Soc. Am. B. **20**, 1491-1502 (2003).
5. D. McMillen, T. D. Hudson, J. Wagner, and J. Singleton, "Holographic recording in specially doped lithium niobate crystals," Opt. Express **2**, 491-502 (1998), http://www.opticsexpress.org/abstract.cfm?URI=OPEX-2-12-491.
6. G. W. Burr, C. M. Jefferson, H. Coufal, M. Jurich, J. A. Honagle, R. M. Macfarlane, and R. M. Shelby, "Volume holographic data storage at areal density of 250 gigapixels/in^2," Opt. Lett. **26**, 444-446 (2001).
7. Y. Yang, I. Nee, K. Buse, and D. Psaltis, "Ionic and electronic dark decay of holograms in $LiNbO_3$:Fe crystals," Appl. Phys. Lett. **78**, 4076–4078 (2001).
8. Y. Yang, K. Buse, and D. Psaltis, "Photorefractive recording in $LiNbO_3$:Mn," Opt. Lett. **27**, 158–160 (2002).
9. T. Volk, N. Rubinina, and M. Wöhlecke, "Optical-damage-resistant impurities in lithium niobate," J. Opt. Soc. Am. B. **11**, 1681-1687 (1994).
10. T. Volk, M. Wöhlecke, N. Rubinina, N. V. Razumovski, F. Jermann, C. Fischer, and R. Bower, "$LiNbO_3$ with the damage -resistant impurity indium," Appl. Phys. A. **60**, 217-225 (1995).
11. N.Y. Kamber, J. Xu, S.M. Mikha, G. Zhang, S. Liu, G. Zhang, "Threshold effect of incident light intensity for the resistance against the photorefractive light-induced scattering in doped lithium niobate crystals", Opt.Commun.**176**, 91-96 (2000).
12. H. Qiao, J.Xu, Q. Wu, X. Yu, Q. Sun, X. Zhang, G. Zhang, and T. Volk, "An increase of photorefractive sensitivity in In: $LiNbO_3$ crystal," Opt. Mater. **23**, 269-272 (2003).
13. C. Gu, J. Hong, H. Li, D. Psaltis and P. Yeh, "Dynamics of grating formation in photovoltaic media," J. Appl. Phys. **69,** 1167–1172 (1991).
14. Q. He, G. Liu, X. Li, J. Wang, M. Wu, and G. Jin, "Suppression of the influence of a photovoltaic dc field on volume holograms in Fe:$LiNbO_3$," Appl. Opt. **41**, 4104-4107 (2002).
15. K. Peithmann, A. Wiebrock, and K. Buse, "Photorefractive properties of highly doped lithium niobate crystals in the visible and near-infrared," Appl. Phys. B. **68**, 777-784 (1999).
16. G. Zhang, Y. Tomita, X. Zhang, and J.Xu, "Near-infrared holographic recording with quasi-nonvolatile readout in $LiNbO_3$: In, Fe," Appl. Phys. Lett. **81**, 1393-1395 (2002).
17. G. W. Burr, D. Psaltis, "Effect of the oxidation state of $LiNbO_3$:Fe on the diffraction efficiency of multiple holograms," Opt. Lett. **21**, 893-895 (1996).
18. J. Wang, Q. He, G. Jin, and M. Wu, "Holographic storage parametric optimization of the crystal $LiNbO_3$:Fe based on one-center model," Chinese Journal of Lasers, **B11**, 27-33 (2002).
19. Y. Liu, L. Liu, L. Xu, and C. Zhou, "Experimental study of non-volatile holographic storage in doubly- and triply-doped lithium niobate crystals," Opt. Commun. **81**, 47–52 (2000).
20. C. Ouyang, L. Cao, Q. He, Y. Liao, M. Wu, and G. Jin, "Sidelobe suppression in volume holographic optical correlators by use of speckle modulation," Opt. Lett. **28**, 1972-1974 (2003).
21. Y. Liao, Y.Guo, L.Cao, X.Ma, Q.He, and G.Jin, "Experiment on parallel correlated recognition of 2030 human faces based on speckle modulation," Opt.Express **12**, 047-4052 (2004), http://www.opticsexpress.org/abstract.cfm?URI=OPEX-12-17-4047.
22. D. Psaltis, D. Brady, and K. Wagner, "Adaptive optical networks using photorefractive crystals," Appl. Opt. **27**, 1752-1759 (1988).